https://doi.org/10.1051/epjconf/202327704008

1.5 MW CW RF Loads for Gyrotrons

Lawrence Ives[1] , *Thuc* Bui[1], *Thomas* Habermann[1], *George* Collins[1], *David* Marsden[1], *Jeffrey* Neilson[2], *Tim* Horn[3], *and Chris* Rock[3]

[1]Calabazas Creek Research, Inc., 690 Port Drive, San Mateo, CA 94404 USA
[2]Lexam Research, 10 Black Fox Way, Redwood City, 24062 CA US
[3]North Carolina State University, 915 Partners Way, Raleigh, NC 27695 USA

Abstract. A new series of MW-class, RF loads were developed that can dissipate power levels exceeding 1.5 MW at frequencies from 28 GHz to 180 GHz. The new loads are designed to reflect less than 0.25% of the input power and operate continuously (CW). Stainless-steel and anodized aluminum versions were developed. The stainless steel version is designed to meet requirements for nuclear facilities, such as ITER, while the aluminum version is capable of power levels exceeding 2 MW CW. The aluminum version is also lighter and less expensive. This paper describes the design and capabilities of the loads.

1 Introduction

Electron cyclotron resonant heating (ECRH) is an important mechanism for increasing the temperature of tokamak plasmas. In addition to plasma heating, RF power is used for current drive and suppression of plasma instabilities. Gyrotrons provide the RF power for these and other applications and generate hundreds of kilowatts to more than 1.5 MW of long pulse or continuous wave (CW) power. Several organizations provide MW-class gyrotrons producing 1 MW or more from 110 GHz to 170 GHz. ITER specifications indicate gyrotrons producing 1.5 MW will eventually be required, and 2 MW sources are envisioned for DEMO.

Development and operation of gyrotrons requires loads to dissipate the RF power. Calabazas Creek Research, Inc. (CCR) developed the first load capable of dissipating more than 1.25 MW CW in the late 1990s [1]. CCR delivered these loads to Europe, Japan, Korea, and the United States and several are still operational. These loads accept RF power in a Gaussian mode transmitted in waveguide or free space.

In 2012, CCR completed development of 2 MW CW loads supporting RF input in 60.3mm or 63.5mm waveguide. In addition to supporting higher power, these loads reduced reflected power to less than 1% [2]. Three loads were delivered to QST in Japan, and one was used to test the 1.9 MW, 110 GHz gyrotron at JT-60A [3]. The loads have dissipated tens of thousands of pulses of 1 MW or more, and no arcs or thermal failures have been reported. In fact, CCR is not aware of any gyrotron test that was prematurely terminated by a CCR load in over twenty years of operation.

Several issues have been addressed over the years. The 1.25 MW loads suffered from persistent water leaks around rotating seals. This issue was eliminated with improve seals in the mid-2000s. These loads also exhibited more than 5% reflected power, which was addressed in the 2 MW loads. The 2 MW loads also incorporated ferromagnetic seals that increased performance and reliability.

Fig. 1. 1.5 MW CW RF load

The new load, shown in Fig. 1, was designed to improve reliability and reduce cost by eliminating rotating components and leveraging additive manufacturing to improve performance. The development also focused on dramatically reducing reflected power and accommodating increased mode impurities in the RF input. Estimated reflected power is less than 0.25%.

CCR developed two, new, load versions. Many facilities, such as ITER, place strict limits on materials for vacuum and wetted surfaces. CCR's 1.25 and 2 MW load cylinders were fabricated using anodized aluminum to leverage the relatively low weight and high thermal conductivity. This material is prohibited by many fusion research facilities, so CCR developed a load primarily fabricated from stainless steel (SST) and copper. Consequently, this load is significantly heavier and more expensive than previous loads. The reduced thermal conductivity of SST also reduces the maximum power capability to 1.5 MW CW. To accommodate other users, CCR developed an anodized aluminum version capable of higher power at reduced cost and weight. This version also leverages additively manufactured (AM) components not currently qualified for nuclear facilities. The following sections describe design and fabrication of the loads and provide simulations of the RF and thermomechanical performance.

2 Mechanical design

The principal innovation in CCR loads is active distribution of the RF beam to uniformly distribute the power and eliminate arcing. All loads capable of MW operation incorporate overmoded cavities where the power is absorbed. This results in constructive and destructive interference from reflected RF waves. When constructive interference occurs near a load surface, it causes excessive RF heating and subsequent outgassing. The associated high electric field can initiate an arc that damages the surface or terminates gyrotron operation. CCR's concept eliminates this occurrence by continuously sweeping the power. The effectiveness of this approach has been confirmed over twenty years of operation where no load arcs or thermal damage have been reported.

The 1.25 MW loads used a rotating mirror at the downstream end of the load to sweep the power; however, this reflected the RF wave back toward the input, resulting in significant reflected power. This was essentially eliminated in the 2MW loads, which used a launcher at the input to sweep the beam. The launch angle was chosen such that the input was shadowed from reflected power by the back side of the launcher. This reduced reflected power from the load to approximately 0.7%, as measured by QST, and confirmed by General Atomics. This achieved the specification that reflected power be less than 1%.

To increase performance and reliability and reduce cost, CCR explored alternatives to rotating components for the RF sweeping. While effective, the cost and complexity of ferromagnetic seals was problematic. The new design uses a bellows to support an internal reflector that sweeps the RF power without rotating. The reflector is revolved around the input in the configuration shown in Fig 2.

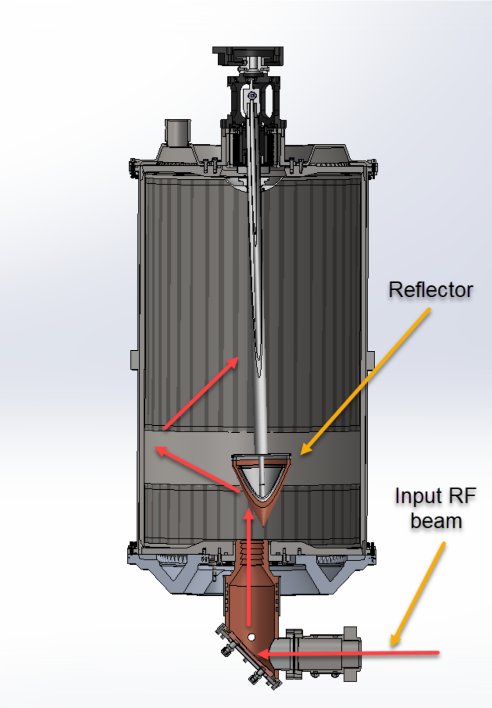

Fig. 2. Conceptual mechanical design

This approach provides several advantages. Probably the most important is cost. The ferromagnetic seals in the 2 MW loads cost more than 4,000 USD and requires precision support structures. The bellows and its support components cost less than 1,500 USD. Because the bellows is deflected less than 1.5°, the stresses are far below yield levels, implying unlimited lifetime. The reduced complexity also lowers assembly cost.

CCR tested this design using the setup shown in Fig 3. The assembly operated more than 4,000 cycles over 315 hours. This is almost three times the required lifetime specified by ITER. It was still operating nominally when testing was terminated due to schedule constraints. The horizontal test configuration was chosen to maximize stresses on the assembly.

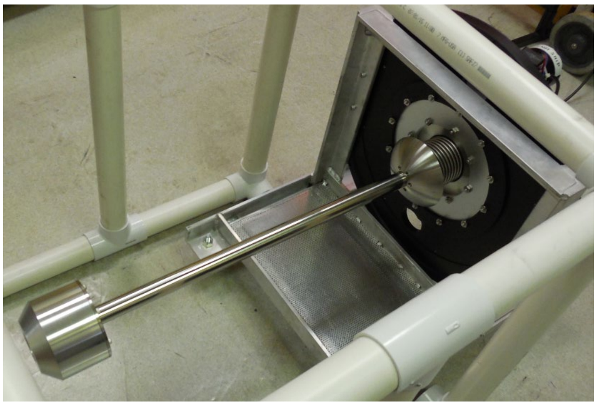

Fig 3. Life test of bellows-based reflector assembly

3 Input coupler

Reflected power is a critical issue for gyrotron users, as excessive levels can impact gyrotron operation and potentially result in catastrophic failure. A key task was reducing reflected power, hopefully below measurable levels. The design incorporates a focusing miter bend that accepts the input beam from corrugated waveguide and focuses it through a reduced size aperture, as shown in **Fig. *4***. The corrugated input waveguide terminates at the flange where the RF beam is launched and expands as a Gaussian, free space mode.

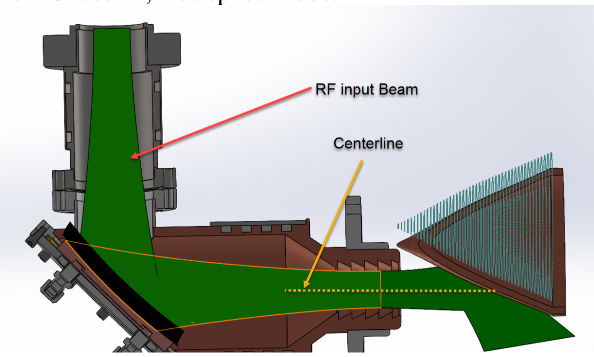

Fig. 4. RF beam path through input coupler

The input coupling system was designed using Surf3d. **Fig. *6*** shows the RF beam path from the end of the corrugated transmission line, past the miter bend, through the final aperture to the revolving reflector, and through two bounces on the load cylinder walls. The simulation also provides the power density profiles for thermomechanical analyses and cooling system design.

CCR also investigated load operation in the presence of non HE_{11} input modes. The concern is that power in these modes may be trapped in the input coupler before entering the main load. Any RF power propagating into the cylindrical section of the load will be scattered and absorbed. For proper operation, a significant amount of non-HE_{11} power must be transmitted into the main load by the miter mirror. If this is achieved, there is high confidence that low reflected power can be achieved, even with significant input mode impurities. CCR simulated non-HE_{11} modes, specifically, the HE_{12}, HE_{13},

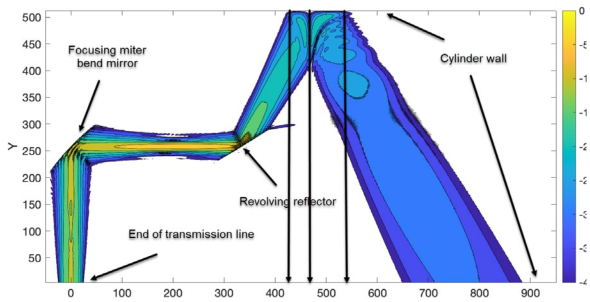

Fig. 5. Surf3d simulation of RF beam path into load

HE_{21}, HE_{22}, and HE_{23}. These are the closest modes to the HE_{11} and the most likely to constitute non-HE_{11} power.

Fig. 5 shows the field intensity for the HE_{12} mode. In this configuration, the RF power is launched from a corrugated waveguide at -14 cm in a vertical direction. It impacts the focusing miter mirror and is reflected toward the aperture at location zero on the axis. The far-right boundary is a non-reflecting surface representing the cylindrical section of the load. The aperture at location zero is 20 mm diameter. The reflected power for each mode is determined by numerical integration of **E** x **H** over a circle with the same diameter as the corrugated waveguide and at a position just below the excitation field plane and normalized to the input power to get fractional power reflection (FPR). For the HE_{12} mode the FPR was still quite small at 0.004. In addition, the total power reflected (RPF) was calculated. These results are shown in Table 1. To get total reflected power, the power in each higher mode must be multiplied by the FPR for that mode and summed with reflection phase included. The input mode composition is not known a priori, but assuming 10% of input power is distributed evenly in the five higher order modes and they all add in phase (an unlikely occurrence representing an upper bound in reflection amplitude) the total reflected power would be 0.25%. Since the higher order modes attenuate faster, it is unlikely the power in higher order modes would be equal to the lower order modes, thus it is likely the reflected power would be substantially less since the lower order modes have substantially lower FPR coefficients. The total power reflected (and not coupled to the input waveguide) for assumption of 10% of input power is distributed evenly in the five higher order modes is 1%.

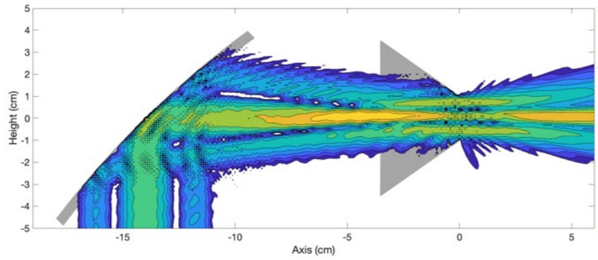

Fig. 6. Field intensity for HE_{12} mode excitation. The incident mode is reflected off focusing mirror, and a small part is reflected back by cone funnel on the axis at 0 cm.

These calculations used a 20 mm diameter aperture. From Fig. 6, one can observe that the maximum radial extent of the HE_{12} fields is less than 20 mm. Consequently, a 40 mm diameter aperture would result in total transmission of this mode into the load cylinder. This would also drastically reduce FPR for the other, higher order modes. The actual load aperture is approximately 44 mm diameter, which further reduces or eliminates reflected power from higher order modes.

Table 1. Fractional Reflection for non-HE11 modes

Mode	FPR	Total Power
HE_{11}	0	.003
HE_{12}	.004	.042
HE_{13}	.047	.143
HE_{21}	.002	.019
HE_{22}	.009	.0443
HE_{23}	.063	.286

There are two issues associated with the higher order modes. One is the level of reflection back into the input waveguide, and the other is the power that fails to enter the waveguide and is dissipated in the coupler region. The analysis above indicates total reflected power for

10% non-HE_{11} modes would be 1%. This is within the cooling capability of the input coupler.

CCR anticipates less than 0.25% of the RF power will be reflected into the transmission line and sufficient cooling is available to dissipate this absorbed power. Note that any higher mode power coupled back into the input waveguide will be rapidly dissipated due to waveguide loss. Consequently, the corrugated waveguide input should be well cooled.

The heat load on the miter bend mirror exceeds that of all other surfaces and is typically the component limiting the power capability of the load. It is fabricated from copper chrome zirconium (CuCrZr), which supports higher power densities than copper. It is also well cooled. For 1.2 MW CW operation, a 26 LPM flow rate results in a vacuum wall temperature of 122° C and wet wall temperature of 73° C. The peak stress is approximately 1/3 the yield stress. Higher coolant flow will allow higher power operation. Provided sufficient cooling, it is anticipated that 2 MW CW operation can be supported.

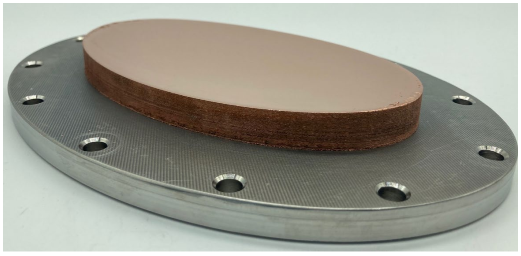

Fig. 7. 3D printed miter mirror assembly

It should be noted that the power density on the mirror is reduced by expansion of the Gaussian beam in the input section of the load. Consequently, the power density will be less than on miter bends in the incoming transmission line. The power delivered to the load will most likely be determined by transmission line components rather than load components.

Fig. 8. Solid model of input coupler for 170 GHz operation with 63.5 mm waveguide

ITER specifications prohibit braze joints in the vacuum envelope, so the initial mirror was explosively bonded to the stainless steel support plate. North Carolina State University (NCSU) used additive manufacturing (AM) to build this assembly by 3D printing CuCrZr directly on the support plate. An advantage with this technique, in addition to dramatically lowering cost, includes integration of cooling channels closer to the vacuum surface with increased thermal transfer to the coolant. This could allow higher power operation than available with explosive bonding. Surface finishes achieved with AM are currently unacceptable for most RF applications due to the inherent roughness. This is avoided by machining the reflective surface following printing. The roughness remains on the interior cooling channels, but this enhances heat transfer at appropriate flow rates. Fig. 7 shows a miter mirror assembly built using AM. The machined copper reflecting surface exhibits a mirror-quality finish while the sides show the inherent roughness from printing.

The load design incorporates several features to reduce reflected power. First, the revolving reflector shadows the input from RF waves propagating parallel to the input axis. Stepped walls at the aperture will reflect any incident power back into the cylindrical section of the load. Secondly, only power that impacts the miter mirror at a precise angle will be focused into the input transmission line. Given the input path for reflected power, the probability of this is quite low. Power incident on the mirror at the wrong angle will impact the walls of the stainless steel, smooth bore waveguide, which is well cooled. Only power entering the corrugated waveguide parallel to its axis can propagate back to the gyrotron.

Fig. ***8*** shows the input coupler model for 170 GHz operation. The assembly includes ports for vacuum pumping and an arc detector. All components are water cooled.

Fig. 9. Solid model of the reflector assembly

4 Reflector assembly

RF power enters the load cylinder through the input assembly and impacts the revolving cone of the reflector assembly, shown in Fig. 9**.** The cone revolves around the input coupler every two seconds and evenly distributes the thermal loading while preventing arcing from constructive interference. Water cooling is provided through the support shaft, which also scatters the RF power around the load interior. The cone surface is shaped to maximize axial and azimuthal scattering of the RF beam. An electric motor revolves the cone using a chain drive. CCR has used the same model electric motor for more than twenty years, and none has ever failed. The drive gear is interlocked to ensure the cone is properly revolving prior to injection of RF power.

The full power of the RF beam impacts the cone, but the area of impact moves around the cone surface as it revolves around the input. Consequently, the primary concern is cyclic fatigue. CCR used the incident power density obtained from Surf3d to analyze the thermomechanical performance using a cyclic profile. Fig. 10 shows the relevant temperatures as a function of time for a 30 LPM coolant flow rate. The peak stresses are well below the 44 MPa yield stress, implying unlimited lifetime due to thermal fatigue.

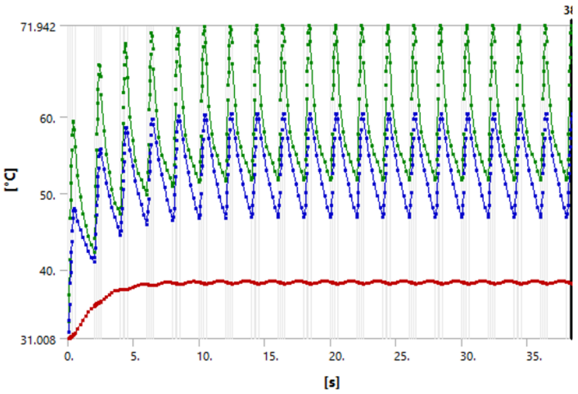

Fig. 10. Vacuum wall (green), average (blue), and wet wall (red) temperatures for reflector cone

5 Load Cylinder

The input coupler and reflector assemblies are common to both the stainless steel and aluminum versions of the load cylinder assembly. The primary function of the cylinder assembly is to absorb the input RF power and transfer the energy to the coolant. This assembly includes the high flow cooling circuit and provides the primary vacuum envelope for the load.

Fig. 11. Stainless steel inner cylinder

The inner cylinder assembly consists of the inner cylinder, shown in Fig. 11, with end plates electron beam welded (EBW) to the ends. The interior of the cylinder includes RF loss material to increase absorption in regions of low to moderate power density. CCR uses plasma sprayed PP-146 compound to increase the RF loss in these regions [4]. This material is 97% titanium dioxide. The exterior is grooved to enhance heat transfer to the coolant. The end plates support the input and output coolant manifolds for the primary coolant and provide the interfaces to the input coupler and reflector assembly. Fig. 12 shows the stainless steel version, which weighs approximately 300 kg. Forgings for the load cylinders, both stainless steel and aluminum, are centrifugally spun, which avoids stresses that can cause warping after machining.

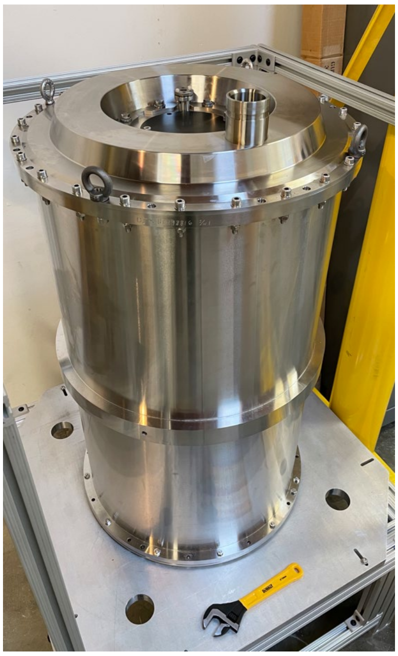

Fig. 12. Stainless steel load cylinder assembly

The primary cooling circuit consists of manifold end plates and an outer cylinder. These components are attached to the inner cylinder using bolts and O-ring seals.

CCR analyzed the thermal performance using power densities determined from the Surf3d simulation shown in **Fig. *6*** and the two second periodicity of the rotating beam. The polarization with highest RF loss was used in all cases. Fig. 13 shows the power density profile at the wall for 1.5 MW operation, and Fig. 14 shows the maximum inner wall temperature, which peaks below 62°C. Note that the cylinder reaches steady state operation after approximately twenty seconds. The peak stress is less than 170 MPa, well below the yield stress

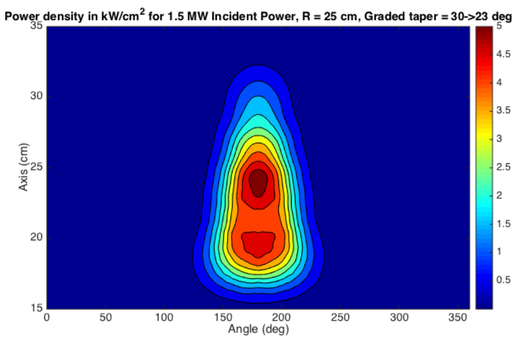

Fig. 13. RF power density on cylindrical wall for 1.5 MW input power

of 262 MPa. This indicates the load can operate indefinitely (CW) under these conditions.

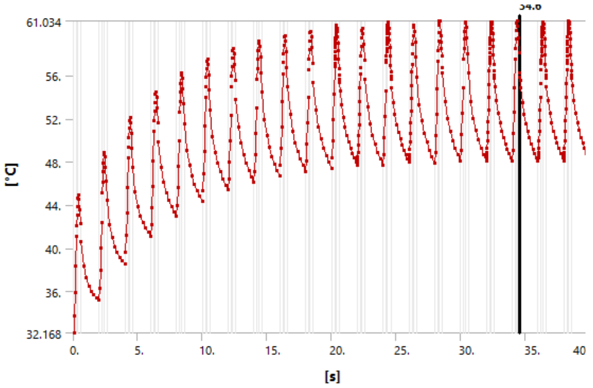

Fig. 14. Maximum inner wall temperature through forty seconds of operation

The anodized aluminum version of the assembly is slightly longer than the SST version due to thicker, e-beam welded end plates. The outer cylinder and end plates are also anodized aluminum. The weight of this assembly is less than 200 kg and lower cost than the stainless steel version. The increased thermal conductivity allows operation to more than 2 MW CW. The thermal analysis was presented in reference [2].

6 Diagnostics and control system

CCR developed a control system based on programmable logic controllers (PLCs) that monitors the system, controls load operation, and uses temperature and flow sensors to calculate and display dissipated power in real time. The system includes the associated plumbing, sensors, and cables. It also provides an interlock signal to confirm that the load is operating correctly and a digital interface for remote control and data acquisition. Specifically, the system provides the following:

Fig. 15. Diagnostic and control system, including PLC controller, plumbing, and sensors

- Controls reflector motor,
- Measures reflector revolution rate,
- Measures reflector, input coupler, and main coolant flow rates,
- Monitors inlet and outlet coolant temperatures,
- Calculates and displays average and peak RF power for short pulse, long pulse or CW operation,
- Provides interlocks for main coolant flow and reflector revolution,
- Includes emergency Off button
- Provides digital I/O (Modbus) for remote monitoring and control

A front panel touch screen provides user control and display of operational and performance parameters. Fig. 16 shows a photo of the PLC controller, temperature and flow sensors, cables, and a portion of the plumbing hardware included with the system. A sample display is shown in Fig. 16.

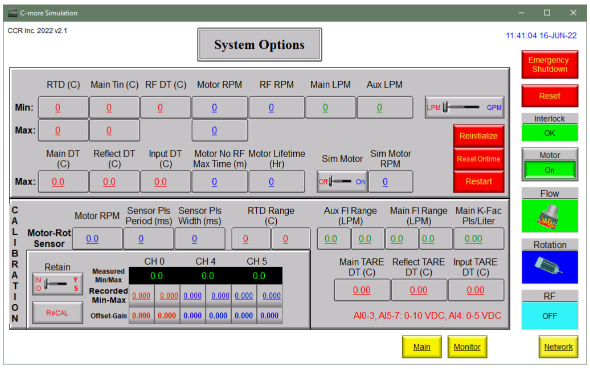

Fig. 16. Sample PLC display

7 Summary

Calabazas Creek Research, Inc. is continuing to develop high power RF loads for the ECE-ECRH and gyrotron community. The new loads offer improved capability, increased reliability, and lower cost. Both stainless steel and anodized aluminum load cylinders are available with the aluminum version offering higher power operation, significant weight reduction, and reduced cost. The diagnostics and control system provides temperature, flow, and dissipated power data in real time and remote data acquisition and control.

References

1. R. L. Ives, M. Mizuhara, R. Schumacher, R. Pendleton, “Development of a High Power CW Waterload for Gaussian Mode Gyrotrons,” IEEE Trans. Plasma Sci., Vol. 27, No. 2, April 1999.
2. R.L. Ives, M. Mizuhara, t. Kobayashi, S. Moriyama, g. Collins, P. Borchard, and Jeff Neilson, “Design and Operation of a 2-MW CW RF Load for Gyrotrons,” IEEE Trans. Electron Devices, Vol. 61, No. 6, June 2014.
3. T. Kobayashi, QST-Japan, Private communications, May 2022.
4. Available from Aimtek, Inc., 201 Washington Street, Auburn MA 01501 USA